Effects of Hexagonal Boron Nitride Sheets on the Optothermal Performances of Quantum Dots-Converted White LEDs

Shuling Zhou, Bin Xie, Yupu Ma, Wei Lan, and Xiaobing Luo, *Fellow, IEEE*

***Abstract*— Recently, quantum dots-converted white light-emitting diodes (QDs-WLEDs) are attracting numerous attention due to their high luminous efficiency and excellent color quality. As for color conversion material, the quantum dots (QDs) are commonly embedded into a low-thermal-conductivity polymer matrix. In this case, their generated heat during the photoluminescence process can hardly be dissipated into the heat sink, leading to a high working temperature and reduced lifetime. Adding particles with high thermal conductivity to the QDs layer can enhance its thermal conductivity, and thus reduce QDs' working temperature. At the same time, these particles may affect the optical properties of QDs. However, this problem has still not been deeply studied. In this article, we systematically investigated the effects of the highly thermal-conductive hexagonal boron nitride sheets (hBNSs) on the optothermal performances of QDs/phosphor film in white light-emitting diodes (WLEDs). The thermal conductivity of QDs/phosphor film was significantly increased by 24% after adding 5wt% of 45-μm-diameter hBNS. As for the optical performance, the transparency of the silicone gel film with 45-μm-diameter hBNS was much better than that with 6–9-μm-diameter hBNS under the same weight fraction. Furthermore, the scattering effect of hBNS plays a more important role in enhancing the light conversion performance of QDs than that of phosphor. At last, a color stability test showed the increasing rate of correlated color temperature (IRCCT) of hBNS-added WLEDs are 21% smaller than that of common WLEDs after working 153 h, meaning a better QDs stability in hBNS-added WLEDs.**

***Index Terms*— Hexagonal boron nitride sheets (hBNSs), light conversion, quantum dots (QDs), thermal conductivity.**

I. Introduction

QUANTUM dots-converted white light-emitting diodes (QDs-WLEDs) have attracted researchers' attention and become a potential alternative for the next-generation artificial light sources, due to their advantages over conventional light sources, such as high color rendering index (CRI), wide color gamut, and simple manufacturing technics [1]–[5]. Specifically, compared with the traditional inorganic phosphors [6], Quantum dots (QDs) have unique optical properties, such as very narrow full-width at half-maximum (FWHM) of 10–30 nm, quite high absolute quantum yield of 90%, and the size-tunable emission spectra covering the ultraviolet-visible-infrared wavelength region [7]–[9]. In spite of all these favorable characteristics, QDs are sensitive to temperature and totally quenched when the temperature exceeded 140 °C, which was irreversible [10]. The thermal degradation and quenching happening under high working temperature hinder the wide application of QDs-WLEDs. Woo *et al.* [11] found that the high working temperature in the QDs-WLEDs had resulted from the thermal accumulation effect inside the QDs. For example, when the QDs' mass weight fractions were 0.2%, 0.6%, and 1%, the temperatures rose to 94 °C, 109 °C, and 131 °C, respectively. It was inferred from the case of phosphor-converted LEDs (pc-LEDs) [12]–[16] that the heat generated from the process of QDs light conversion was hardly dissipated to heat sink due to the low thermal conductivity of the colloid surrounding the QDs.

Some researchers have proposed chemical modification [17], metal doping [18], surface coating [19], and mesoporous embodying [20] to improve QDs' thermal stability. However, these strategies inevitably lead to a decrease in the luminous efficiency of QDs. Alternatively, another method to protect the QDs from the damage of high working temperature by reinforcing the thermal conductivity of the QDs-polymer film was presented. Zheng *et al.*[21] used the electrostatic spinning technology to dope the QDs colloids into fibrous films, whose thermal conductivity was increased by 40% and the working temperature was reduced from 146 °C to 138 °C. Xie *et al.* [22] successfully reduced the working temperature of QDs from 127.2 °C to 104.5 °C by making a compound structure of QDs and hexagonal boron nitride sheets (hBNSs), which has a high aspect ratio and a highly anisotropic thermal property [23]. It is reasonable for utilizing hBNS as the thermal enhancement filler in optomaterial of electronic devices because of the negligible light absorption due to the intrinsic white color, the low coefficient of thermal expansion and the electrically insulating property [24]–[26]. Therefore, hBNS will not cause serious optical energy loss that happens to

Manuscript received June 4, 2019; revised August 21, 2019; accepted August 21, 2019. Date of publication September 9, 2019; date of current version October 29, 2019. This work was supported in part by the National Natural Science Foundation of China under Grant 51625601, Grant 51576078, and Grant 51606074, in part by the Ministry of Science and Technology of the People's Republic of China under Grant 2017YFE0100600, and in part by the Creative Research Groups Funding of Hubei Province under Grant 2018CFA001. The review of this paper was arranged by Editor C. Surya. *(Corresponding author: Xiaobing Luo.)*

The authors are with the School of Energy and Power Engineering, Huazhong University of Science and Technology, Wuhan 430074, China (e-mail: luoxb@hust.edu.cn).

Color versions of one or more of the figures in this article are available online at http://ieeexplore.ieee.org.

Digital Object Identifier 10.1109/TED.2019.2937340

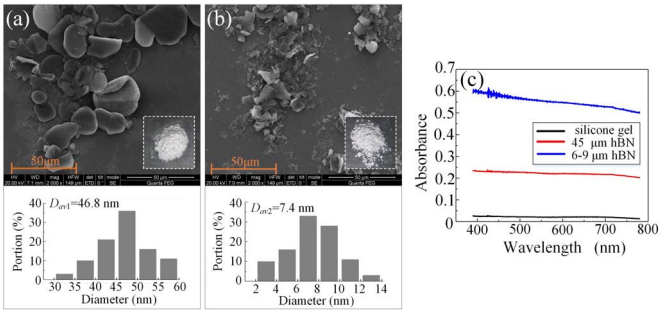

Fig. 1. Scanning electron microscope images and scale histograms of (a) 45-μm-diameter hBNS and (b) 6–9-μm-diameter hBNS and (c) their absorbance spectra of composite films tested by ultraviolet-visible light divider lambda 35.

other reinforcing fillers such as graphene [27], metal [28], and carbon nanotube [29]. However, the influence of hBNS on the optical and thermal performances of QDs film has not been deeply investigated.

Therefore, in this article, we experimentally studied the influence of hBNS on the luminescence performance of phosphor, QDs of the composite photo-luminescent colloid film, proving that hBNS with an optimal diameter and a low weight fraction can be utilized to produce QDs-WLEDs with qualified optical properties as well as high thermal stability.

II. Experiments

A. Property of hBN

In this article, considering that the varied average diameters of hBNS may lead to different performances of the translucency and heat transportability of composite film, two kinds of hBNS with a maximum difference in particle size supplied by Momentive Performance Materials Inc. were used as the filling materials. Their surface morphologies are shown in Fig. 1(a) and (b). According to their product specification [30], the average diameters are 45 and 6–9 μm, respectively, which are testified by the corresponding scale histograms in Fig. 1. Fig. 1(c) is the absorbance spectra of silicone gel composite films at 1.5 mm of thickness with hBNS of 5% weight fraction of two varied sizes, respectively.

B. hBN-Added Pure Silicone Gel Film

We tested a series of silicone gel films consisting of two kinds of hBNS with weight fractions of 5% and 10%, respectively. For testing the optical power emitting from the film, as shown in Fig. 2(a), we used a remote configuration, in which the film and the chip are on two ends of a reflector cup with a height of 8 mm. The cylindrical film has a diameter of 10 mm and a thickness of 1.45 $\pm$ 0.05 mm.

The translucency was determined by the ratio of the optical powers of the hBNS-added silicone gel film to that of the silicone gel film. An integrating sphere (Everfine, ATA-1000) was used to test the optical power, and the driving current of the LED was set as 20 mA. The thermal diffusivity of the film was measured by a laser flash method (Netzsch LFA 457).

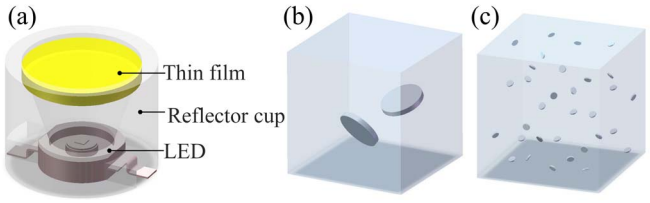

Fig. 2. (a) Test model of the remote encapsulation WLEDs. Distribution schematics of hBNS in (b) Sample a1 and (c) Sample b1.

TABLE I
Weight Fractions of Varied Components in the Silicone Gel Composite Films

component		phosphor	QDs	hBNS
A	1	0	0	0
	2	0	0	5%
	3	0	0	10%
B	1	10%	0	0
	2	10%	0	5%
	3	10%	0	10%
C	1	0	0.025%	0
	2	0	0.025%	5%
	3	0	0.025%	10%
D	1	10%	0.025%	0
	2	10%	0.025%	5%
	3	10%	0.025%	10%

C. hBN-Added Light-Converting Film

To study the scattering and absorption effects of hBNS on the light conversion performances of yellow-emissive phosphor and red-emissive QDs, we tested the emission spectra, excitation spectra, and optical powers of the different-component silicone gel films and analyzed their heat generations. To realize a WLEDs with a blue LED chip, a color conversion film consisting of silicone gel, red-emissive CdSe/ZnS core-shell QDs, and yellow-emissive $Y_3Al_5O_{12}:Ce^{3+}$ (YAG:Ce) phosphor was prepared. The white light was realized by combining the blue light from the LED chip, yellow light from the phosphor, and red light from QDs. As shown in Table I, four different combinations of optical components in the films were Samples A1-3: pure silicone gel as a reference, Samples B1-3: phosphor, Samples C1-3: QDs, and Samples D1-3: phosphor and QDs, respectively. As shown in Table I, the weight fractions of phosphor and QDs were 10% and 0.025%, respectively; and the weight fractions of 45-μm hBNS were 5% and 10%, respectively. The size of films and the driving current of LED were the same as the above cases. The ambient temperature was 25 °C. Besides the optical performance, the thermal diffusivities of Samples D1-3 (QDs/phosphor films) under varied temperatures and the color stability of WLED with the same films on driving current of 300 mA were tested.

III. Results and Discussion

A. Effects of hBNS on Translucency and Heat Diffusion

The values of translucency and thermal diffusivity of four samples of hBNS-silicone gel films shown in Fig. 3 with

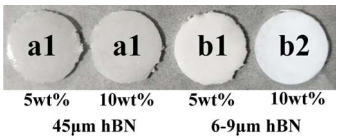

Fig. 3. Films with varied kinds and concentrations of hBNS.

TABLE II
THERMAL DIFFUSIVITY AND TRANSMISSION OF hBNS-ADDED SILICONE GEL FILMS

Sample	a1	a2	b1	b2
Diameter of hBNS (μm)	45		6-9	
Weight fraction of hBNS	5%	10%	5%	10%
Transmission	0.829	0.877	0.414	0.454
Thermal diffusivity (m^2/s)	0.144	0.227	0.108	0.129

TABLE III
EFFECTS OF hBNS ON PEAK INTENSITY OF BLUE, YELLOW, AND RED LIGHT

Sample	A2	A3	B2	B3	C2	C3	D2	D3
Blue	-26%	-33%	-62%	-69%	-51%	-67%	-71%	-79%
Yellow	--	--	0%	-9%	--	--	-14%	-25%
Red	--	--	--	--	+60%	+89%	+47%	+37%

different sizes and weight fractions are listed in Table II. The best translucency was owned by the Sample a1 with 5wt% of 45-μm hBNS, and its thermal diffusivity was also larger than that of Sample b1 with 5 wt% of 6–9 μm hBNS. For understanding the difference between these two cases, the microscopic distribution schematics of hBNS in the matrix are shown in Fig. 2(b) and (c) for Samples a1 and b1, respectively. As we can see, the particle number of Sample a1 was far less than that of Sample b1 under the same weight fraction, which might mean a less scattering of light and a guarantee of better translucency of Sample a1 [31]. As for the thermal diffusivity enhancement, large-diameter particles in Samples a1-2 were more efficient to build the heat transporting channels [32]. In summary, a better translucency and thermal diffusivity of the film were both achieved by adding larger-diameter hBNS at the same low weight fraction.

B. Effects of hBNS on Photoluminescence

Based on the above results, we chose the larger-diameter hBNS (45 μm) as the thermal enhancement material and studied its scattering effect on the optical performance of WLEDs. Fig. 4(a) and (b) are the daylight and ultraviolet light pictures of all the samples in Table I.

The emission spectra of these four kinds of films with different loadings of hBNS are shown in Fig. 5. The peak wavelengths of blue, yellow, and red light were 453, 529, and 633 nm, respectively. The peak intensity changes after adding hBNS are listed in Table III. In Fig. 5(a)–(d), the peak

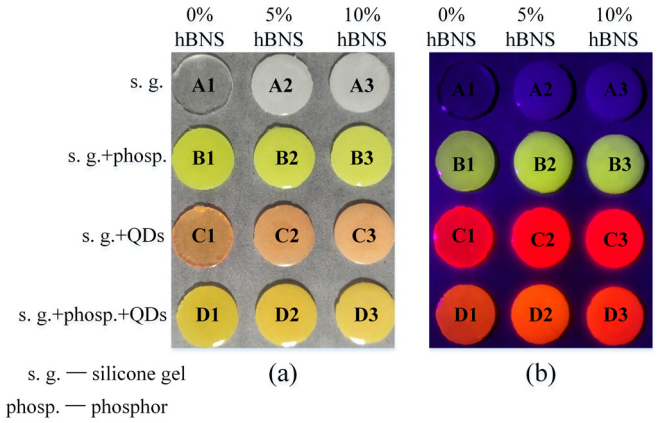

Fig. 4. Varied films under (a) daylight and (b) ultraviolet light.

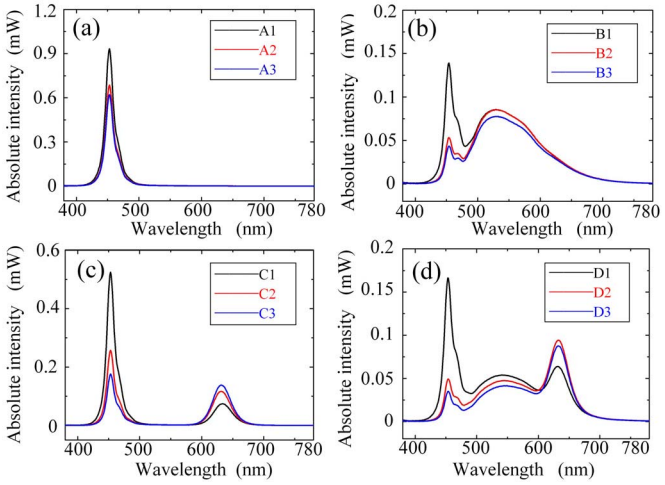

Fig. 5. Emission spectra of different films. (a) Samples A1-3. (b) Samples B1-3. (c) Samples C1-3. (d) Samples D1-3.

intensities of blue light were all reduced after adding hBNS. For example, in Samples A3 and D3, the peak intensities of blue light were decreased by 33% and 79%, respectively. However, the yellow light in Sample B2 shared the same peak intensity with that of the Sample B1, which indicated that adding hBNS enhanced the photoluminescence performance of phosphor due to the hBNS in Sample B2 also have uniform absorption characteristic, shown in Fig. 1(c). Furthermore, the peak intensity of red light increased a lot, such as by 89% and 79% in Samples C3 and D3, respectively.

The excitation spectra of Samples B1-3 (phosphor) and Samples C1-3 (QDs) are shown in Fig. 6. The peak wavelengths of excitation light of phosphor and QDs were 457 and 467 nm, respectively, which maintain after adding hBNS. The relative excitation intensities of Samples B1-3 decreased after adding hBNS, while Samples C1-3 increased. This result accorded with the above emission spectra in Fig. 5(b) and (c). Specifically, in Sample B, the absorption effect of hBNS might be stronger than its scattering effect on the light, which caused the decrease of excitation intensity.

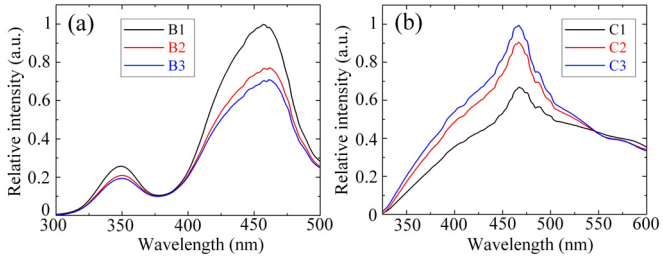

Fig. 6. Excitation spectra of different films. (a) Samples B1-3. (b) Samples C1-3.

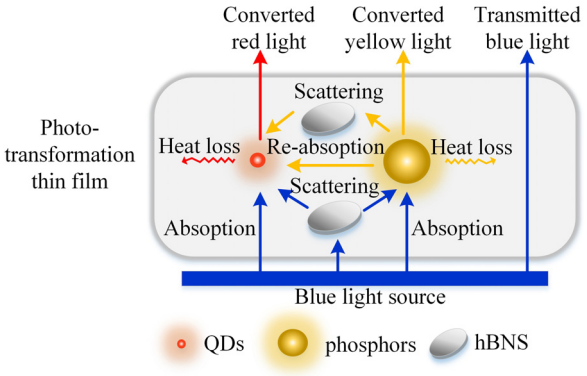

Fig. 7. Schema of the scattering effect of hBNS on the light conversion process of phosphor and QDs.

In short, the existence of a certain amount of hBNS in the films was proven to enhance the emission performance of both phosphors and QDs. It was surprising that the light-conversion performance of QDs got much more increase by adding hBNS in the film. In the following, we have some discussions on it.

To discuss the effects of hBNS on the photoluminescence properties of color conversion materials, we drew a schematic of the light conversion mechanism of a photo-transformation and thermal-enhancement films with QDs, phosphor, and hBNS, as shown in Fig. 7. The blue light partly transmits through the film, and the rest of it is absorbed by the QDs and phosphor. Meanwhile, some yellow light from the phosphor was reabsorbed by QDs. Compared to the without-hBNS case, the scattering effect of hBNS can increase the probability of the blue and yellow light hitting QDs, and also that of the blue light hitting the phosphor [31], causing the enhancement of the photoluminescence performance of QDs and phosphor, as shown in Fig. 5(b)–(d). On the other hand, based on the Mie theory, smaller particles like QDs give more backscattering than bigger particles like phosphors, so that the red light from QDs can raise more than yellow light from phosphor when the same light refracts from hBNS surfaces.

C. Effects of hBNS on Heat Loss and Thermal Conductivity

The effect of hBNS on heat loss needs to be analyzed because it would make no sense if the addition of hBNS caused more heat loss in the film than the enhancement that the thermal diffusion can transfer. Based on the emission spectra

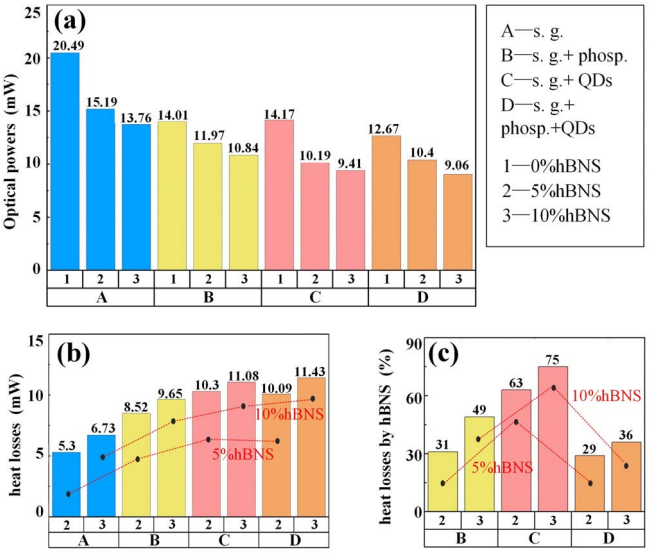

Fig. 8. Different films'. (a) Optical powers. (b) Heat losses. (c) Increased heat losses by adding hBNS.

of different films in Fig. 5, we obtained the corresponding optical powers and conducted a discussion on the heat loss problem.

Fig. 8(a) shows the optical powers of films. In the without-hBNS cases, Samples B1, C1, and D1, the main heat loss was generated by the photoluminescence materials like phosphor and QDs. In the with-hBNS cases shown in Fig. 8(b), the heat loss came not only from the light conversion process but also the absorption and scattering results of hBNS. On the one hand, the hBNS slightly absorbed the visible light, as shown in Fig. 1(c), producing a part of the heat loss ultimately. On the other hand, the scattering effect of hBNS benefited light conversion as discussed above; namely, more heat loss came after more light conversion. The percentages of increased heat losses by adding hBNS in Samples B2-3, C2-3, and D2-3 are shown in Fig. 8(c). The increased heat losses in Samples B2 and C2 with only one kind of photoluminescence particles reached up to 31% and 63%, respectively. In a word, the heat loss caused by adding hBNS was worthy because of the corresponding improvements of the photoluminescence performances of QDs and phosphor.

The thermal conductivities of Samples D1-3 with QDs, phosphor, and hBNS at different temperatures are shown as the solid lines in Fig. 9, which rose continually with increasing weight fractions of hBNS. At 65 °C, the thermal conductivities of Samples D2 and D3 were increased by about 24% and 55%, respectively. In addition, the variation of thermal conductivity as a function of temperature was changed by adding hBNS. For example, the thermal conductivity of Sample D1 at 65 °C was smaller than that of the same film at 80 °C, while there was a reverse in Samples D2-3 whose thermal conductivities at 65 °C were larger than that at 80 °C. Furthermore, as the dashed lines show in Fig. 9, at 65 °C, the QDs/phosphor films had the biggest thermal enhancements after adding hBNS.

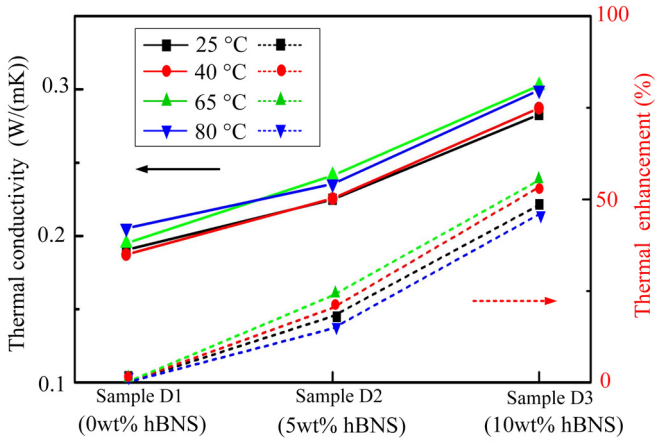

Fig. 9. Thermal conductivity and thermal enhancement of Samples D1-3 under different temperatures.

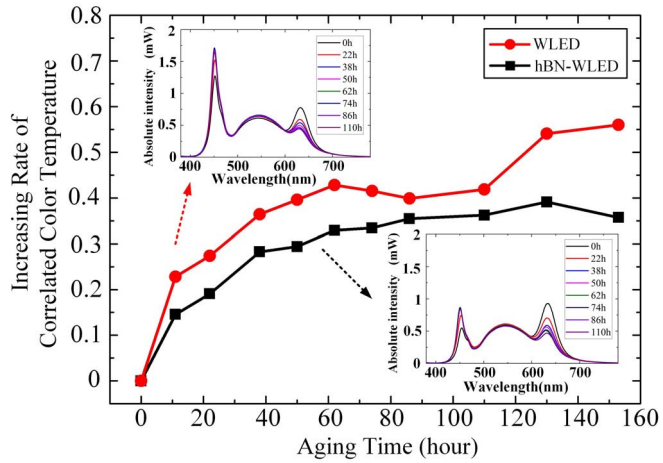

Fig. 10. Aging curves of IRCCT of WLEDs and hBNS-WLEDs. Inset: top-left and bottom-right are the absolute intensity spectra of varied aging time of WLEDs and hBNS-WLEDs, respectively.

D. Effects of hBNS on Stability of QDs-WLEDs

The stability test results of hBNS-WLEDs (Sample D2) and common WLEDs (Sample D1) under continual working time are shown in Fig. 10. Its inter figures on the top-left and bottom-right are the absolute intensity spectra of WLEDs and hBNS-WLEDs, respectively, which both showed the obvious decrease of red-light intensity and increase of blue-light intensity during aging. The change of spectra attested the luminescence decay of QDs in the two aging WLEDs. However, it also implied that the change of their luminous efficiency, kind of integral of the spectrum, was unfit to reflect the luminescence decay of QDs. But their correlated color temperatures (Tc(x), x is the aging time in hours) increase apparently after aging, simply due to the QDs failure. The aging curves of the increasing rate of correlated color temperature [IRCCT, equal to Tc(x)/Tc(0)-1] in Fig. 10 showed a better comparison of the QDs stability between the hBNS-WLEDs and the common WLEDs. After working 153 h, the IRCCT of hBNS-WLEDs was 21% smaller than that of common WLEDs, proving that adding hBNS in QDs layer can improve the QDs stability of QDs-WLEDs.

IV. Conclusion

In this article, we experimentally studied the effects of hBNS with quite high thermal conductivity on the luminescence performance of the QDs/phosphor colloid film. The thermal conductivity of QDs/phosphor film was significantly increased by 24% after adding 5wt% of 45-μm-diameter hBNS. Both the thermal diffusivity and translucency of the silicone gel film with large-diameter hBNS were better than that of the small-diameter at the same weight fraction. Furthermore, through analyzing the emission spectra, optical powers, and heat generations of different-components films in WLEDs, we found that the addition of hBNS in the film played a more important role to enhance the light conversion performance of QDs than that of phosphor. Finally, a stability test showed the IRCCT of hBNS-WLEDs is 21% smaller than that of common WLEDs after working for 153 h. This article proves that the thermally conductive hBNS actually facilitates the optical and thermal performances of QDs/phosphor film, which lays a foundation for fabricating highly thermal-conductive QDs composite luminescence materials with excellent optical parameters.

References

[1] S. Nizamoglu, G. Zengin, and H. V. Demir, "Color-converting combinations of nanocrystal emitters for warm-white light generation with high color rendering index," *Appl. Phys. Lett.*, vol. 92, no. 3, Jan. 2008, Art. no. 031102. doi: 10.1063/1.2833693.

[2] K.-S. Cho *et al.*, "High-performance crosslinked colloidal quantum-dot light-emitting diodes," *Nature Photon.*, vol. 3, pp. 341–345, Jun. 2009. doi: 10.1038/nphoton.2009.92.

[3] S. Kim, S. H. Im, and S.-W. Kim, "Performance of light-emitting-diode based on quantum dots," *Nanoscale*, vol. 5, no. 12, pp. 5205–5214, Apr. 2013. doi: 10.1039/C3NR00496A.

[4] R. Zhu, Z. Luo, H. Chen, Y. Dong, and S.-T. Wu, "Realizing Rec. 2020 color gamut with quantum dot displays," *Opt. Express*, vol. 23, no. 18, Sep. 2015, Art. no. 247206. doi: 10.1364/OE.23.023680.

[5] B. Xie, R. Hu, and X. Luo, "Quantum dots-converted light-emitting diodes packaging for lighting and display: Status and perspectives," *J. Electron. Packag.*, vol. 138, no. 2, 2016, Art. no. 020803. doi: 10.1115/1.4033143.

[6] C. C. Lin and R.-S. Liu, "Advances in phosphors for light-emitting diodes," *J. Phys. Chem. Lett.*, vol. 2, no. 11, pp. 1268–1277, May 2011.

[7] S. Kim *et al.*, "Highly luminescent InP/GaP/ZnS nanocrystals and their application to white light-emitting diodes," *J. Amer. Chem. Soc.*, vol. 134, no. 8, pp. 3804–3809, Feb. 2012. doi: 10.1021/ja210211z.

[8] S. Jun, J. Lee, and E. Jang, "Highly luminescent and photostable quantum dot silica monolith and its application to light-emitting diodes," *ACS Nano*, vol. 7, no. 2, pp. 1472–1477, Jan. 2013. doi: 10.1021/nn3052428.

[9] Q. Hong, K.-C. Lee, Z. Luo, and S.-T. Wu, "High-efficiency quantum dot remote phosphor film," *Appl. Opt.*, vol. 54, no. 15, pp. 4617–4622, May 2015. doi: 10.1364/AO.54.004617.

[10] Y. Zhao, C. Riemersma, F. Pietra, R. Koole, C. de Mello Donegá, and A. Meijerink, "High-temperature luminescence quenching of colloidal quantum dots," *ACS Nano*, vol. 6, no. 10, pp. 9058–9067, Sep. 2012. doi: 10.1021/nn303217q.

[11] J. Y. Woo, K. N. Kim, S. Jeong, and C.-S. Han, "Thermal behavior of a quantum dot nanocomposite as a color converting material and its application to white LED," *Nanotechnology*, vol. 21, no. 49, Nov. 2010, Art. no. 495704. doi: 10.1088/0957-4484/21/49/495704.

[12] X. Luo, X. Fu, F. Chen, and H. Zheng, "Phosphor self-heating in phosphor converted light emitting diode packaging," *Int. J. Heat Mass Transf.*, vol. 58, nos. 1–2, pp. 276–281, Mar. 2013. doi: 10.1016/j.ijheatmasstransfer.2012.11.056.

[13] X. Luo, R. Hu, S. Liu, and K. Wang, "Heat and fluid flow in high-power LED packaging and applications," *Prog. Energy Combustion Sci.*, vol. 56, pp. 1–32, Sep. 2016. doi: 10.1016/j.pecs.2016.05.003.

[14] B. Xie *et al.*, "Structural optimization for remote white light-emitting diodes with quantum dots and phosphor: Packaging sequence matters," *Opt. Express*, vol. 24, no. 26, pp. A1560–A1570, Dec. 2016. doi: 10.1364/OE.24.0A1560.

[15] Y. P. Ma, R. Hu, X. J. Yu, W. C. Shu, and X. B. Luo, "A modified bidirectional thermal resistance model for junction and phosphor temperature estimation in phosphor-converted light-emitting diodes," *Int. J. Heat Mass Transf.*, vol. 106, pp. 1–6, Mar. 2017. doi: 10.1016/j.ijheatmasstransfer.2016.10.058.

[16] Y. Ma, W. Lan, B. Xie, R. Hu, and X. Luo, "An optical-thermal model for laser-excited remote phosphor with thermal quenching," *Int. J. Heat Mass Transf.*, vol. 116, pp. 694–702, Jan. 2018. doi: 10.1016/j.ijheatmasstransfer.2017.09.066.

[17] N. Tomczak, D. Jańczewski, M. Han, and G. J. Vancso, "Designer polymer–quantum dot architectures," *Prog. Polym. Sci.*, vol. 34, no. 5, pp. 393–430, 2009. doi: 10.1016/j.progpolymsci.2008.11.004.

[18] B. Zhao, X. Yao, M. Gao, K. Sun, J. Zhang, and W. Li, "Doped quantum dot@silica nanocomposites for white light-emitting diodes," *Nanoscale*, vol. 7, no. 41, pp. 17231–17236, Aug. 2015. doi: 10.1039/c5nr04839g.

[19] S. T. Selvan, T. T. Tan, and J. Y. Ying, "Robust, non-cytotoxic, silica-coated CdSe quantum dots with efficient photoluminescence," *Adv. Mater.*, vol. 17, no. 13, pp. 1620–1625, Jul. 2005. doi: 10.1002/adma.200401960.

[20] B. Xie *et al.*, "Realization of wide circadian variability by quantum dots-luminescent mesoporous silica-based white light-emitting diodes," *Nanotechnology*, vol. 28, no. 42, Sep. 2017, Art. no. 425204. doi: 10.1088/1361-6528/aa82d7.

[21] H. Zheng, X. Lei, T. Cheng, S. Liu, X. Zeng, and R. Sun, "Enhancing the thermal dissipation of a light-converting composite for quantum dot-based white light-emitting diodes through electrospinning nanofibers," *Nanotechnology*, vol. 28, no. 26, Jun. 2017, Art. no. 265204. doi: 10.1088/1361-6528/aa72d6.

[22] B. Xie *et al.*, "Targeting cooling for quantum dots in white QDs-LEDs by hexagonal boron nitride platelets with electrostatic bonding," *Adv. Funct. Mater.*, vol. 28, no. 30, Jun. 2018, Art. no. 1801407. doi: 10.1002/adfm.201801407.

[23] C. Yuan, B. Duan, L. Li, B. Xie, M. Huang, and X. Luo, "Thermal conductivity of polymer-based composites with magnetic aligned hexagonal boron nitride platelets," *ACS Appl. Mater. Interfaces*, vol. 7, no. 23, pp. 13000–13006, May 2015. doi: 10.1021/acsami.5b03007.

[24] W.-L. Song *et al.*, "Polymer/boron nitride nanocomposite materials for superior thermal transport performance," *Angew. Chem. Int. Ed.*, vol. 51, no. 26, pp. 6498–6501, 2012. doi: 10.1002/anie.201201689.

[25] J. Yin, X. Li, J. Zhou, and W. Guo, "Ultralight three-dimensional boron nitride foam with ultralow permittivity and superelasticity," *Nano Lett.*, vol. 13, no. 7, pp. 3232–3236, Jun. 2013. doi: 10.1021/nl401308v.

[26] X. Zeng, L. Ye, S. Yu, R. Sun, J. Xu, and C.-P. Wong, "Facile preparation of superelastic and ultralow dielectric boron nitride nanosheet aerogels via freeze-casting process," *Chem. Mater.*, vol. 27, no. 17, pp. 5849–5855, 2015.

[27] G. Lian *et al.*, "Vertically aligned and interconnected graphene networks for high thermal conductivity of epoxy composites with ultralow loading," *Chem. Mater.*, vol. 28, no. 17, pp. 6096–6104, Aug. 2016. doi: 10.1021/acs.chemmater.6b01595.

[28] M. Poostforush and H. Azizi, "Superior thermal conductivity of transparent polymer nanocomposites with a crystallized alumina membrane," *Express Polym. Lett.*, vol. 8, no. 4, pp. 293–299, 2014. doi: 10.3144/expresspolymlett.2014.32.

[29] M. Wang *et al.*, "Crack-free and scalable transfer of carbon nanotube arrays into flexible and highly thermal conductive composite film," *ACS Appl. Mater. Interfaces*, vol. 6, no. 1, pp. 539–544, Dec. 2014. doi: 10.1021/am404594m.

[30] *PolaraTherm* Boron Nitride Filler PT110 and PT180.* Accessed: Sep. 2012. [Online]. Available: https://www.momentive.com/zh-cn/categories/ceramics/boron-nitride

[31] H. C. van de Hulst, *Light Scattering by Small Particles*. New York, NY, USA: Wiley, 1957.

[32] S. Kemaloglu, G. Ozkoc, and A. Aytac, "Properties of thermally conductive micro and nano size boron nitride reinforced silicon rubber composites," *Thermochim. Acta*, vol. 499, nos. 1–2, pp. 40–47, Nov. 2010. doi: 10.1016/j.tca.2009.10.020.